

# NATIONAL ADVISORY COMMITTEE FOR AERONAUTICS

REPORT No. 795

## THE NACA IMPACT BASIN AND WATER LANDING TESTS OF A FLOAT MODEL AT VARIOUS VELOCITIES AND WEIGHTS

By SIDNEY A. BATTERSON

DEPARTMENT OF COMMERCE  
Approved for public release  
by Distribution Unit



FIELD COPY  
Science and Technology Project  
Library of Congress  
TO BE RETURNED

LIBRARY OF CONGRESS  
SCIENCE & TECHNOLOGY PROJECT  
TECHNICAL INFORMATION SECTION  
23 DEC 1947

19960813 065

1944

copy # 4

23 DEC 1947

# DISCLAIMER NOTICE



**THIS DOCUMENT IS BEST QUALITY AVAILABLE. THE COPY FURNISHED TO DTIC CONTAINED A SIGNIFICANT NUMBER OF PAGES WHICH DO NOT REPRODUCE LEGIBLY.**

# AERONAUTIC SYMBOLS

## 1. FUNDAMENTAL AND DERIVED UNITS

|             | Symbol | Metric  |                   | English                                     |                   |
|-------------|--------|---|-------------------|---|-------------------|
|             |        | Unit  | Abbrevia-<br>tion | Unit  | Abbrevia-<br>tion |
| Length..... | $l$    | meter.....  | m                 | foot (or mile).....                         | ft (or mi)        |
| Time.....   | $t$    | second.....   | s                 | second (or hour).....                       | sec (or hr)       |
| Force.....  | $F$    | weight of 1 kilogram.....                           | kg                | weight of 1 pound.....                      | lb                |
| Power.....  | $P$    | horsepower (metric).....                            |                   | horsepower.....                             | hp                |
| Speed.....  | $V$    | {kilometers per hour.....<br>meters per second..... | kph<br>mps        | miles per hour.....<br>feet per second..... | mph<br>fps        |

## 2. GENERAL SYMBOLS

|       |  |        |  |
|-------|--|--------|--|
| $W$   | Weight = $mg$  | $\nu$  | Kinematic viscosity  |
| $g$   | Standard acceleration of gravity = 9.80665 m/s <sup>2</sup><br>or 32.1740 ft/sec <sup>2</sup>  | $\rho$ | Density (mass per unit volume)   |
| $m$   | Mass = $\frac{W}{g}$   |        | Standard density of dry air, 0.12497 kg-m <sup>-4</sup> -s <sup>2</sup> at 15° C<br>and 760 mm; or 0.002378 lb-ft <sup>-4</sup> sec <sup>2</sup> |
| $I$   | Moment of inertia = $mk^2$ . (Indicate axis of<br>radius of gyration $k$ by proper subscript.) |        | Specific weight of "standard" air, 1.2255 kg/m <sup>3</sup> or<br>0.07651 lb/cu ft   |
| $\mu$ | Coefficient of viscosity   |        |  |

## 3. AERODYNAMIC SYMBOLS

|       |  |            |   |
|-------|--|------------|---|
| $S$   | Area   | $i_w$      | Angle of setting of wings (relative to thrust line)   |
| $S_w$ | Area of wing   | $i_t$      | Angle of stabilizer setting (relative to thrust<br>line)  |
| $G$   | Gap  | $Q$        | Resultant moment  |
| $b$   | Span   | $\Omega$   | Resultant angular velocity  |
| $c$   | Chord  | $R$        | Reynolds number, $\rho \frac{Vl}{\mu}$ where $l$ is a linear dimen-<br>sion (e. g., for an airfoil of 1.0 ft chord, 100 mph,<br>standard pressure at 15°C, the corresponding<br>Reynolds number is 935, 400; or for an airfoil<br>of 1.0 m chord, 100 mps, the corresponding<br>Reynolds number is 6,865,000) |
| $A$   | Aspect ratio, $\frac{b^2}{S}$                                  | $\alpha$   | Angle of attack   |
| $V$   | True air speed   | $\epsilon$ | Angle of downwash   |
| $q$   | Dynamic pressure, $\frac{1}{2}\rho V^2$                        | $\alpha_0$ | Angle of attack, infinite aspect ratio  |
| $L$   | Lift, absolute coefficient $C_L = \frac{L}{qS}$                | $\alpha_i$ | Angle of attack, induced  |
| $D$   | Drag, absolute coefficient $C_D = \frac{D}{qS}$                | $\alpha_a$ | Angle of attack, absolute (measured from zero-<br>lift position)  |
| $D_0$ | Profile drag, absolute coefficient $C_{D_0} = \frac{D_0}{qS}$  | $\gamma$   | Flight-path angle   |
| $D_i$ | Induced drag, absolute coefficient $C_{D_i} = \frac{D_i}{qS}$  |            |   |
| $D_p$ | Parasite drag, absolute coefficient $C_{D_p} = \frac{D_p}{qS}$ |            |   |
| $C$   | Cross-wind force, absolute coefficient $C_c = \frac{C}{qS}$    |            |   |

---

## **REPORT No. 795**

---

# **THE NACA IMPACT BASIN AND WATER LANDING TESTS OF A FLOAT MODEL AT VARIOUS VELOCITIES AND WEIGHTS**

**By SIDNEY A. BATTERSON**

**Langley Memorial Aeronautical Laboratory  
Langley Field, Va.**

---

# National Advisory Committee for Aeronautics

*Headquarters, 1500 New Hampshire Avenue NW., Washington 25, D. C.*

Created by act of Congress approved March 3, 1915, for the supervision and direction of the scientific study of the problems of flight (U. S. Code, title 49, sec. 241). Its membership was increased to 15 by act approved March 2, 1929. The members are appointed by the President, and serve as such without compensation.

JEROME C. HUNSAKER, Sc. D., Cambridge, Mass., *Chairman*

LYMAN J. BRIGGS, Ph. D., *Vice Chairman*, Director, National Bureau of Standards.

CHARLES G. ABBOT, Sc. D., *Vice Chairman, Executive Committee*, Secretary, Smithsonian Institution.

HENRY H. ARNOLD, General, United States Army, Commanding General, Army Air Forces, War Department.

WILLIAM A. M. BURDEN, Special Assistant to the Secretary of Commerce.

VANNEVAR BUSH, Sc. D., Director, Office of Scientific Research and Development, Washington, D. C.

WILLIAM F. DURAND, Ph. D., Stanford University, California.

OLIVER P. ECHOLS, Major General, United States Army, Chief of Maintenance, Matériel, and Distribution, Army Air Forces, War Department.

AUBREY W. FITCH, Vice Admiral, United States Navy, Deputy Chief of Operations (Air), Navy Department.

WILLIAM LITTLEWOOD, M. E., Jackson Heights, Long Island, N. Y.

FRANCIS W. REICHELDERFER, Sc. D., Chief, United States Weather Bureau.

LAWRENCE B. RICHARDSON, Rear Admiral, United States Navy, Assistant Chief, Bureau of Aeronautics, Navy Department.

EDWARD WARNER, Sc. D., Civil Aeronautics Board, Washington, D. C.

ORVILLE WRIGHT, Sc. D., Dayton, Ohio.

THEODORE P. WRIGHT, Sc. D., Administrator of Civil Aeronautics, Department of Commerce.

---

GEORGE W. LEWIS, Sc. D., *Director of Aeronautical Research*

JOHN F. VICTORY, LL. M., Secretary

HENRY J. E. REID, Sc. D., Engineer-in-Charge, Langley Memorial Aeronautical Laboratory, Langley Field, Va.

SMITH J. DEFRANCE, B. S., Engineer-in-Charge, Ames Aeronautical Laboratory, Moffett Field, Calif.

EDWARD R. SHARP, LL. B., Manager, Aircraft Engine Research Laboratory, Cleveland Airport, Cleveland, Ohio

CARLTON KEMPER, B. S., Executive Engineer, Aircraft Engine Research Laboratory, Cleveland Airport, Cleveland, Ohio

---

## TECHNICAL COMMITTEES

AERODYNAMICS

OPERATING PROBLEMS

POWER PLANTS FOR AIRCRAFT

MATERIALS RESEARCH COORDINATION

AIRCRAFT CONSTRUCTION

*Coordination of Research Needs of Military and Civil Aviation*

*Preparation of Research Programs*

*Allocation of Problems*

*Prevention of Duplication*

---

LANGLEY MEMORIAL AERONAUTICAL LABORATORY  
Langley Field, Va.

AMES AERONAUTICAL LABORATORY  
Moffett Field, Calif.

AIRCRAFT ENGINE RESEARCH LABORATORY, Cleveland Airport, Cleveland, Ohio

*Conduct, under unified control, for all agencies, of scientific research on the fundamental problems of flight*

---

OFFICE OF AERONAUTICAL INTELLIGENCE, Washington, D. C.

*Collection, classification, compilation, and dissemination of scientific and technical information on aeronautics*

## REPORT NO. 795

# THE NACA IMPACT BASIN AND WATER LANDING TESTS OF A FLOAT MODEL AT VARIOUS VELOCITIES AND WEIGHTS

By SIDNEY A. BATTERSON

### SUMMARY

The first data obtained in the United States under the controlled testing conditions necessary for establishing relationships among the numerous parameters involved when a float having both horizontal and vertical velocity contacts a water surface are presented. The data were obtained at the NACA impact basin. The report is confined to a presentation of the relationship between resultant velocity and impact normal acceleration for various float weights when all other parameters are constant. Analysis of the experimental results indicated that the maximum impact normal acceleration was proportional to the square of the resultant velocity, that increases in float weight resulted in decreases in the maximum impact normal acceleration, and that an increase in the flight-path angle caused increased impact normal acceleration.

### INTRODUCTION

Until the present time, almost all experimental work related to loads on seaplanes landing on water has consisted of full-scale landing tests. Attempts to use results of these full-scale tests to establish relationships among the various impact parameters have not been very successful for two reasons: (1) A prearranged test program involving the isolation of selected parameters could not be carried out since the values for a number of the variables were a function of piloting technique, and the natural conditions of the wind and the sea were not controllable during the test; and (2) the available instruments proved inadequate to supply sufficiently accurate results.

In order to overcome the disadvantages of full-scale testing, an impact basin in which float models could be tested under controlled conditions was constructed at the Langley Memorial Aeronautical Laboratory at Langley Field, Va. The first data obtained in the NACA impact basin, which are contained in the present report, may be used with the results of subsequent investigations to establish basic relationships among the impact parameters. Logical interpretation of results of flight tests investigating conditions beyond the scope of the NACA impact basin will then be possible.

The present tests are confined to establishing a relationship between resultant velocity and impact normal acceleration for seaplanes of various weights. The solution of the

problem of determining landing loads must follow further investigations under controlled conditions in order to isolate the effects of a number of other parameters such as flight-path angle, dead rise, hull shape, and trim.

### SYMBOLS

- $V$  resultant velocity of float, feet per second  
 $V_h$  horizontal velocity component of float, feet per second  
 $V_v$  vertical velocity component of float, feet per second  
 $g$  acceleration of gravity (32.2 ft/sec<sup>2</sup>)  
 $\gamma$  flight-path angle, degrees (see fig. 1)  
 $\tau$  float trim, degrees  
 $n_i$  impact acceleration normal to water surface,  $g$

### DESCRIPTION OF APPARATUS

#### FLOAT MODEL AND NACA IMPACT BASIN

The model consisted of a float designed to conform to exceptionally high strength requirements. Care was exercised during the design and construction of this model to

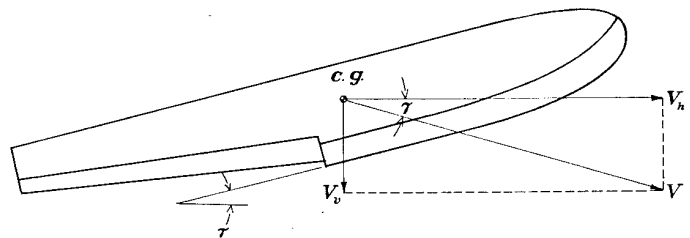


FIGURE 1.—Components of resultant velocity of float.

obtain a reasonably smooth bottom. The sheet-metal skin and most of the structural members were made of dural in order to obtain the minimum weight conforming to the load specifications. The weight of the model was 407 pounds; however, provisions were included whereby 2000 pounds of additional weight could be bolted onto the sides in increments of 25 pounds. The lines and pertinent dimensions of the float model are shown in figure 2. A feature of these lines is the absence of all chine flare.

The NACA impact basin is essentially a concrete tank 360 feet long, 24 feet wide, and 11 feet deep with a normal water depth of 8 feet. Heavy built-up steel rails are suspended along the entire length of the tank with the exception of the

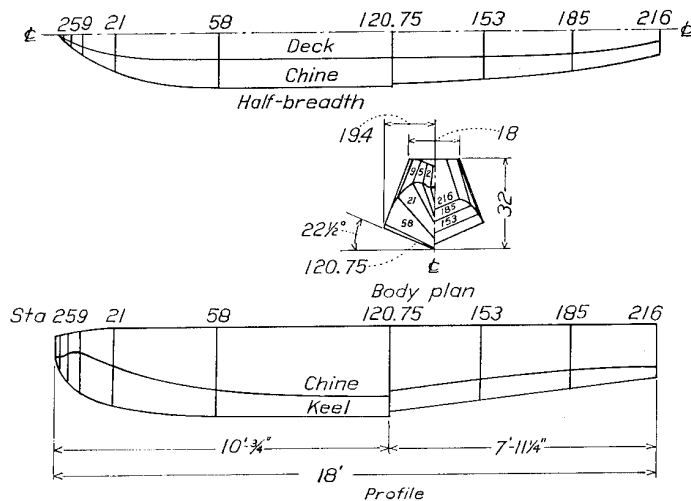


FIGURE 2.—Lines of float model tested in NACA impact basin.

last 40 feet, which is to be occupied by a wave maker. The rails and a portion of the tank are shown in figure 3. The upper, lower, and inner surfaces of each rail were ground straight and parallel within a tolerance of 0.002 inch and the same tolerance was held during installation in locating the rails with respect to each other and to the water surface.

A main carriage embodying a drop linkage to which the model is fastened travels down the tank on the rails. Figure 4



FIGURE 3.—Tank and rails of NACA impact basin.

shows the general arrangement of the carriage with many of the secondary members omitted for clearness. The basic carriage structure consists of chrome-molybdenum steel tubing (fig. 5); the total weight, without model and instruments but including the drop linkage, is approximately 5000 pounds. It may be noted that both lower and upper wheels are provided. The upper wheels are arranged in sets of two and located in trucks which swivel in a vertical plane parallel to the longitudinal carriage center line so that the load is equalized between the two wheels. Solid-rubber instead of pneumatic tires are used to reduce to a minimum deflections under load. Before installation, the outside diameter of each wheel was ground concentric to the axle

bearing and then balanced. The lower wheels may be jacked up against the lower surface of the rails until both upper and lower wheels exert a predetermined pressure on the rails. Oscillations transmitted to the carriage are limited by this arrangement to very small amplitudes and therefore have little disturbing effect upon the actual drop process and the instruments. Lateral restraint is provided by four side wheels bearing upon the inner rail surfaces.

The drop linkage consists of the boom and the upper and lower linkbars, which are pivoted at both ends, and with the

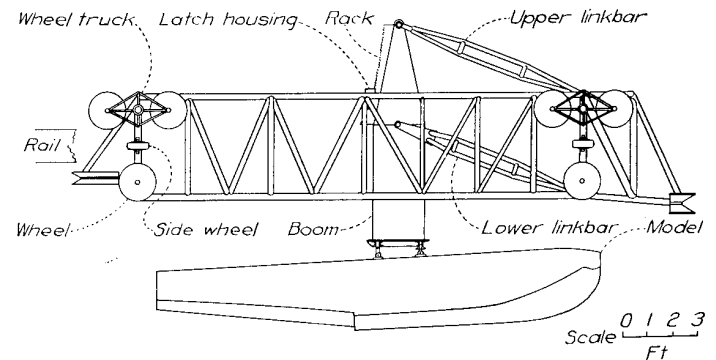


FIGURE 4.—Carriage of NACA impact basin.

boom form a parallelogram type of linkage (fig. 4). The model was fastened rigidly to the lower boom fitting by means of bolts through three lugs built into the float (figs. 6 and 7). By this attachment, the float was restrained in all directions with respect to the boom but had freedom in the vertical direction since it was attached to the parallelogram linkage. The lower boom fitting provides a means for setting the float at various trims and angles of yaw. The float may be dropped from any height up to 4 feet, depending upon the vertical velocity component desired, by engaging the corresponding rack tooth with a latch on the carriage. This latch is released by means of a trip cam located at the proper point along one rail. Releasing the latch allows the boom and the float to drop freely except for the restraint imposed by the upper and lower linkbars, which keep the boom vertical as the float drops. The motion imparted to the model is not perpendicular to the water surface during

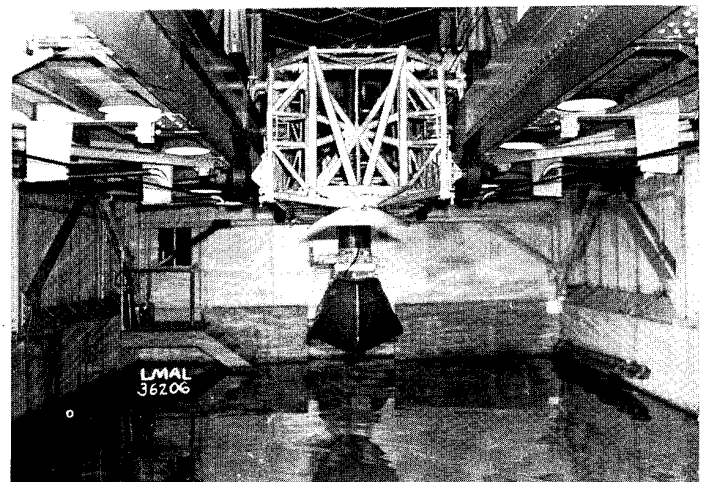


FIGURE 5.—Front view of carriage in NACA impact basin.

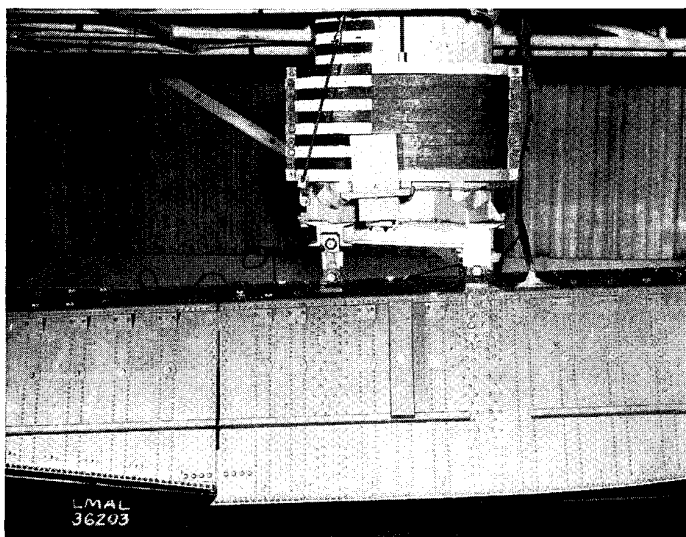


FIGURE 6.—Side view of model fastened to boom in NACA impact basin.

## INSTRUMENTATION

The operation of the horizontal-velocity recorder is dependent upon 1-inch strips of thin metal, referred to as "interrupters," that protrude about 4 inches below the lower inside corner of one rail at 1-foot intervals throughout the length of the tank. These interrupters may be seen on the left rail in figure 8. A photoelectric cell is located on the carriage in such a manner that each interrupter causes a break in the photoelectric-cell circuit as the carriage travels down the tank. The current is then fed to a high-frequency galvanometer element of a recording oscillograph in which a shift occurs in the record line each time the photoelectric-cell circuit is opened by an interrupter. In addition, the oscillograph record contains  $\frac{1}{100}$ -second timing lines. Inasmuch as the carriage is traveling at practically constant

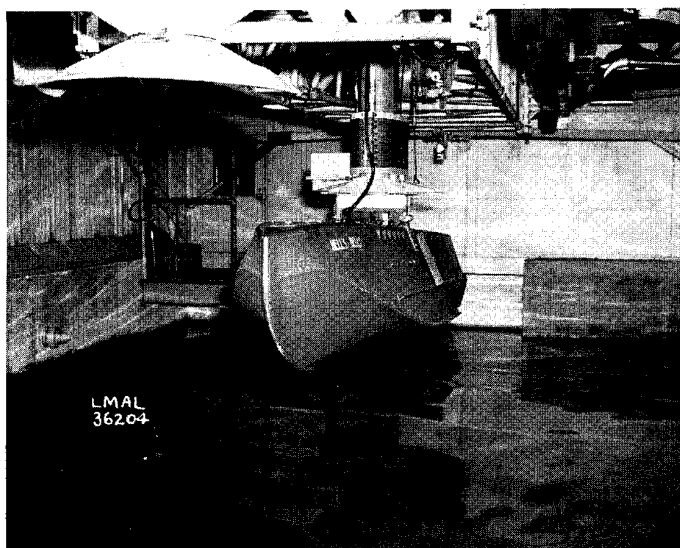


FIGURE 7.—Front view of model fastened to boom in NACA impact basin.

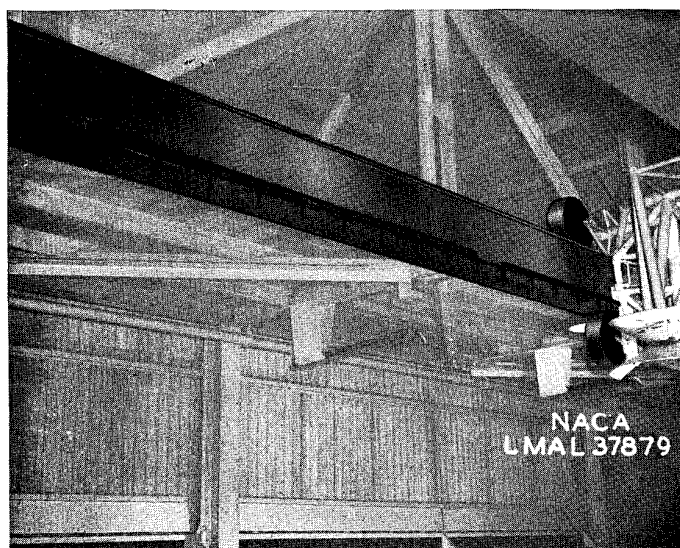


FIGURE 8.—Photoelectric-cell interrupters in NACA impact basin

a large part of the drop. Since the immersion occurs when the linkbars are practically level, however, any horizontal component contributed by the linkage arrangement is at a minimum during impact and is negligible. The dropping weight may be varied by the addition of lead bars fitted around the boom and bolted together as shown in figure 6. The total weight of the boom and linkbars alone, and hence the minimum dropping weight, is 700 pounds.

In order to simulate wing lift, an air-cylinder and piston arrangement that can apply any desired lift on the model up to 2400 pounds is incorporated in the carriage. This mechanism is referred to as the "buoyancy engine." The lift is applied to the model by so connecting the boom and the piston of the buoyancy engine with a cable and sheave system that the piston is forced to travel against the air pressure in the cylinder as the float drops. The amount of lift exerted on the model depends upon the initial air pressure supplied to the cylinder before each run. The rod running upward at an angle from the bottom rear point of the boom (fig. 6) is the lower-end connection of the cable system. With this arrangement the application of the lift may be withheld throughout the downward travel of the boom until just before the float contacts the water. The float is thus allowed to attain the desired vertical velocity component.

The carriage has no self-contained drive but any desired horizontal velocity up to 110 feet per second may be attained by means of a catapulting system. The catapult is of the type used by the Navy on shipboard for launching service planes and accelerates the carriage to the desired speed in a distance of 60 feet. The drop linkage is released at such a point that the impact occurs approximately 100 feet from the point at which the catapult stroke ends. This procedure allows a period during which most of the irregularities and oscillations inherent in the catapult run are damped out. Following the impact, the carriage run is terminated by a Navy arresting gear capable of dissipating the total kinetic energy of the carriage in less than 100 feet.

velocity between the end of the catapult stroke and the impact, this velocity can be determined by dividing the number of interrupters passed during this interval by the time.

The displacement of the boom and its velocity in the vertical direction are also recorded by the oscillograph. The displacement is recorded by a galvanometer element, which deflects in proportion to the amount of current that flows through a piece of resistance wire. The effective length of this wire is varied with the position of the boom by completing the circuit through a sliding contact. The displacement of this contact along the wire follows the boom travel. The same apparatus is used in the determination of the vertical velocity component. In order to determine the vertical velocity component, however, the current derived from the slide wire is directed into several high-capacity condensers and thus electrically differentiated. The galvanometer element records this change in current, which is a function of the boom vertical velocity. The velocity is then derived from the recorded change in current by reference to a suitable calibration curve.

The impact normal accelerations were initially determined with an accelerometer that recorded the flexure of a cantilever vane as measured by a strain gage. The frequency of the accelerometer was 12.5 cycles per second. An amplifying system was required, however, to adapt the accelerometer to the oscillograph that recorded the other values. Since amplifying equipment was not available in time for the tests, a special recorder was necessary for this particular instrument. The records obtained during the first part of the test showed that extraneous vibrations were disturbing the galvanometer element which recorded the impact accelerations. An accelerometer that recorded the angular displacement of an unbalanced galvanometer was therefore substituted for the rest of the test. This instrument had a self-contained optical recording system, had a frequency of 10.5 cycles per second, and was apparently undisturbed by extraneous vibrations. The damping was between five-tenths and six-tenths of the critical damping. The instrument was enclosed in a box and mounted rigidly on the boom between the front and rear float fittings. The mounting may be seen in figures 6 and 7.

#### TEST PROCEDURE

The data presented herein were obtained during the initial calibration runs at the NACA impact basin. The test program thus depended upon the calibration requirements, which necessitated runs at varying weights and landing velocities. A test program was therefore formulated that consisted of a systematic series of runs from which the variation of maximum normal acceleration was obtained as a function of resultant velocity and float weight with all other parameters constant.

The model was tested at dropping weights of 1100, 1500, 1950, and 2400 pounds. A complete series of runs was made for each weight, with horizontal velocities covering an approximate range from 35 to 95 feet per second. An attempt was made to maintain throughout the test a con-

stant ratio of vertical velocity component  $V_v$  to horizontal velocity component  $V_h$ . The value of  $V_v/V_h$  is designated  $\tan \gamma$ , where  $\gamma$  is the flight-path angle. The value of  $\tan \gamma$  was selected as 0.125 for the present tests. In order to check the effect of an increased flight-path angle, four additional runs in which  $\tan \gamma$  was approximately 0.200 were made for the dropping weight of 1100 pounds. The trim was  $3^\circ$  and the angle of yaw was  $0^\circ$  throughout each series. During the impact process, a lift equal to the dropping weight in each case was exerted on the float by means of the buoyancy engine. The normal accelerations were recorded and the maximum value was noted for each run.

#### PRECISION

The apparatus used in the present tests gives measurements that are believed correct within the following limits:

|   |           |
|---|-----------|
| Horizontal velocity, feet per second..... | $\pm 0.5$ |
| Vertical velocity, feet per second.....   | $\pm 0.2$ |
| Acceleration, percent.....                | $\pm 5$   |

The strain-gage accelerometer was used throughout the series in which the dropping weight was 1500 pounds but was replaced by the galvanometer accelerometer for the other three series of tests. The accuracy of  $\pm 5$  percent for acceleration measurements refers to the galvanometer accelerometer. This accuracy represents the extreme limits of error possible throughout the range of applied load frequencies from the static to the natural frequency of the accelerometer and is based upon observations of a frequency-response curve derived experimentally for the instrument. Inasmuch as the test results showed no marked decrease in acceleration values at high-frequency loads, it was concluded that the natural frequency of the accelerometer was not exceeded.

In the lower velocity ranges, the attempt to maintain constant flight-path angle was not very successful, because no calibration data were available and the horizontal velocity components had to be estimated. In addition, deviations occurred between the vertical velocity components expected from drop calibrations made with the carriage at rest and the vertical velocity components obtained during the test runs. The magnitude of these deviations decreased less rapidly than the corresponding vertical velocity components and therefore decreased the accuracy of the flight-path angle less at high than at low velocities.

#### RESULTS AND DISCUSSION

The results of each series of tests for dropping weights of 1100, 1500, 1950, and 2400 pounds are shown as logarithmic plots in figures 9 to 12, respectively. The impact normal accelerations in  $g$  units are derived from the accelerometer record. Inasmuch as the buoyancy engine contributed a force equal to the dropping weight,  $1g$  was subtracted from the values obtained from the accelerometer record to isolate the force resulting from the impact. The results of the four runs for which  $\tan \gamma$  was approximately 0.200 are plotted in figure 9, which clearly indicates that an increase in the flight-path angle increased the normal acceleration.

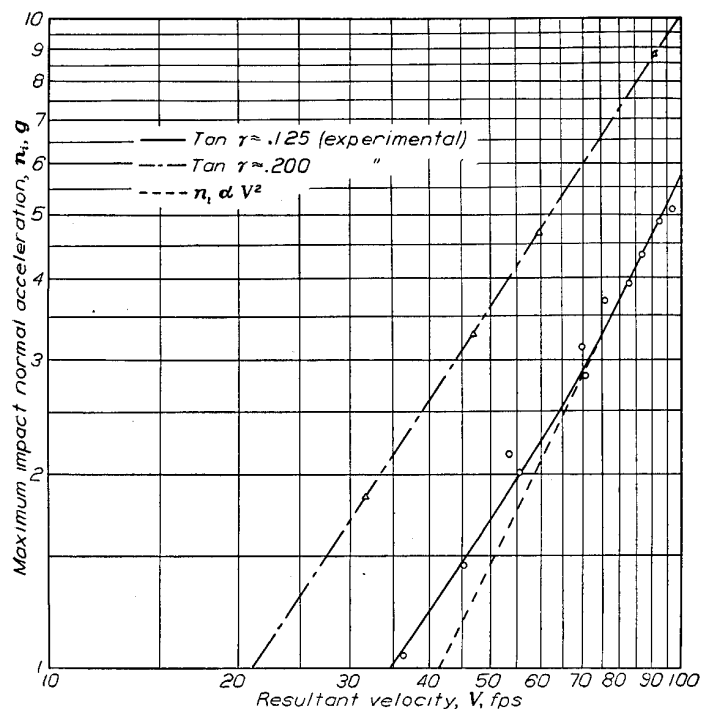


FIGURE 9.—Variation of maximum impact normal acceleration with resultant velocity for float model with dropping weight of 1100 pounds.

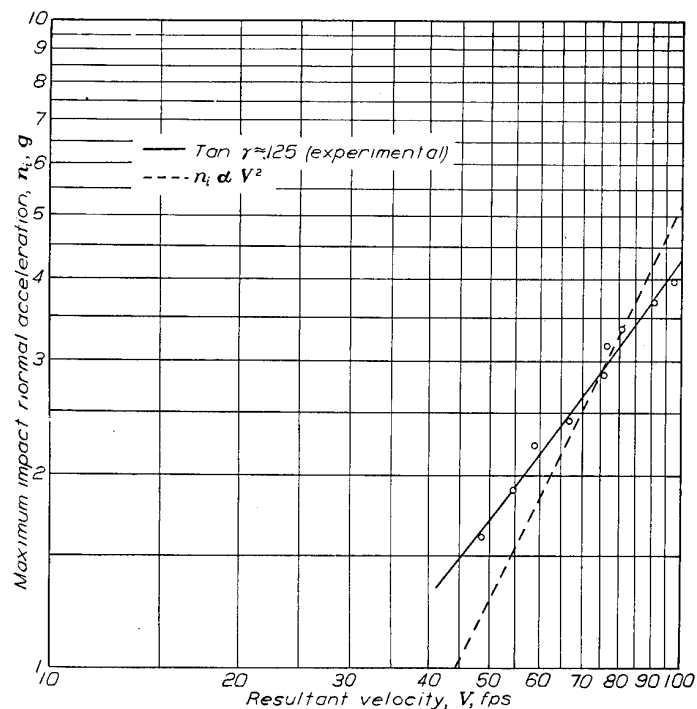


FIGURE 11.—Variation of maximum impact normal acceleration with resultant velocity for float model with dropping weight of 1950 pounds.

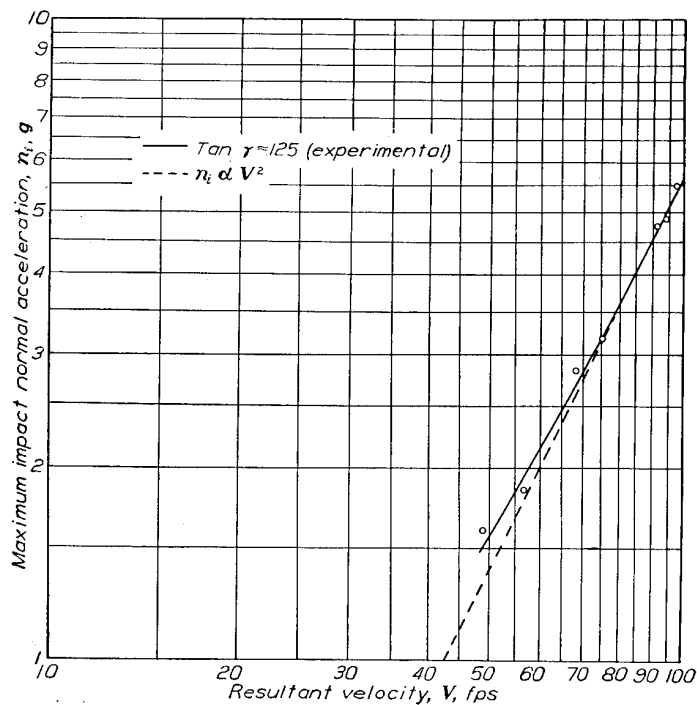


FIGURE 10.—Variation of maximum impact normal acceleration with resultant velocity for float model with dropping weight of 1500 pounds.

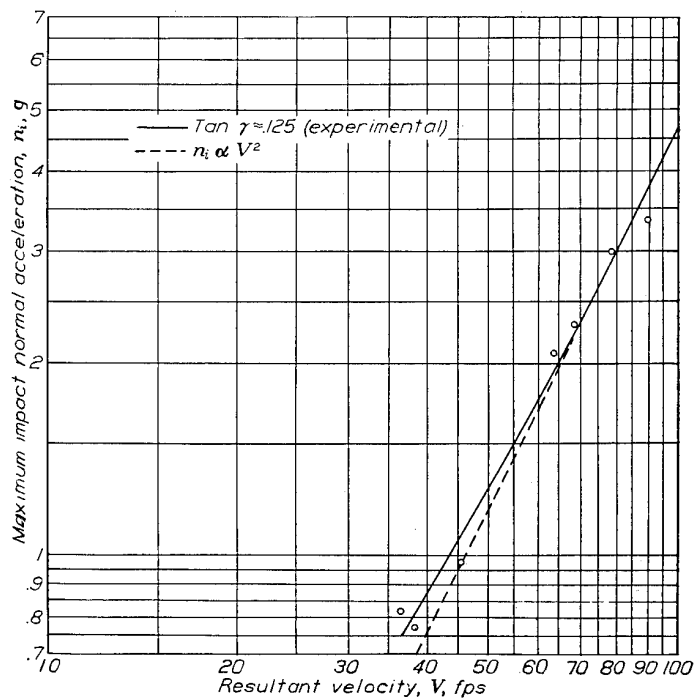


FIGURE 12.—Variation of maximum impact normal acceleration with resultant velocity for float model with dropping weight of 2400 pounds.

The short-dash lines in figures 9 to 12 have slopes that represent the proportion

$$n_i \propto V^2$$

and pass through the experimental points that correspond to  $\tan \gamma \approx 0.125$  as determined from figure 13, which shows the variation in flight-path angle with resultant velocity for the four dropping weights. By referring the faired experimental curve of figure 9 for  $\tan \gamma \approx 0.125$  to figure 13 (a), the maximum normal acceleration can be observed to be directly proportional to  $V^2$  when the flight-path angle remains constant. Below 72 feet per second, however, this proportion no longer holds and the maximum normal accelerations show a larger increase with resultant velocity than is indicated by the line for  $n_i \propto V^2$ . This trend is expected in order to be consistent with the four points of figure 9 that were obtained at  $\tan \gamma \approx 0.200$ . This analysis can be applied to figures 10 and 12 and figures 13(b) and 13(d), respectively, although the range in which the flight-path angle remains constant and the amount by which  $\tan \gamma$  varies differ somewhat in figures 13(b) and 13(d). By applying this analysis to figure 13(c), it would be expected that the values of maximum normal acceleration and resultant velocity that correspond to values of  $V$  from 76 feet per second (the point at which  $\tan \gamma \approx 0.125$ ) to the maximum velocity would show some proportion other than  $V^2$  since the line representing  $\tan \gamma$  has a definite slope within this range of  $V$ ; that is, at  $V > 76$  feet per second, the values of maximum normal acceleration should lie below the curve for  $n_i \propto V^2$  whereas, at  $V < 76$  feet per second, the values of maximum normal acceleration should lie above the curve for  $n_i \propto V^2$ . Figure 11 shows that such is the case. The dashed line for  $n_i \propto V^2$  is determined by the three points in figure 13(c) at which  $\tan \gamma \approx 0.125$ . It thus appears that, provided the flight-path angle is constant, the maximum normal accelerations resulting from the water landing impacts vary directly as the square of the resultant velocities. This conclusion agrees with the Newtonian or  $V^2$  law of fluid resistance since the Reynolds number was very large. The slope of the line through the points for  $\tan \gamma = 0.200$  in figure 9 cannot be relied upon as indicative of the true trend since only four points were obtained and the range of  $\gamma$  was approximately 10 percent.

The dashed lines of figures 9 to 12 are replotted in figure 14, which therefore presents the experimental variation of maximum impact normal acceleration with resultant velocity for various dropping weights with all other parameters constant. It may be noted that the maximum normal acceleration decreases as the weight increases. The curve representing a weight of 1500 pounds shifted, as was mentioned previously, because the galvanometer element that recorded the acceleration for this series of tests was out of balance. Extraneous vibrations were therefore superimposed upon the accelerometer record and accelerations greater than the actual impact accelerations were consequently recorded. No attempt was made to evaluate the decrease in maximum normal acceleration that resulted from the increase in weight since the data appeared inadequate for this purpose.

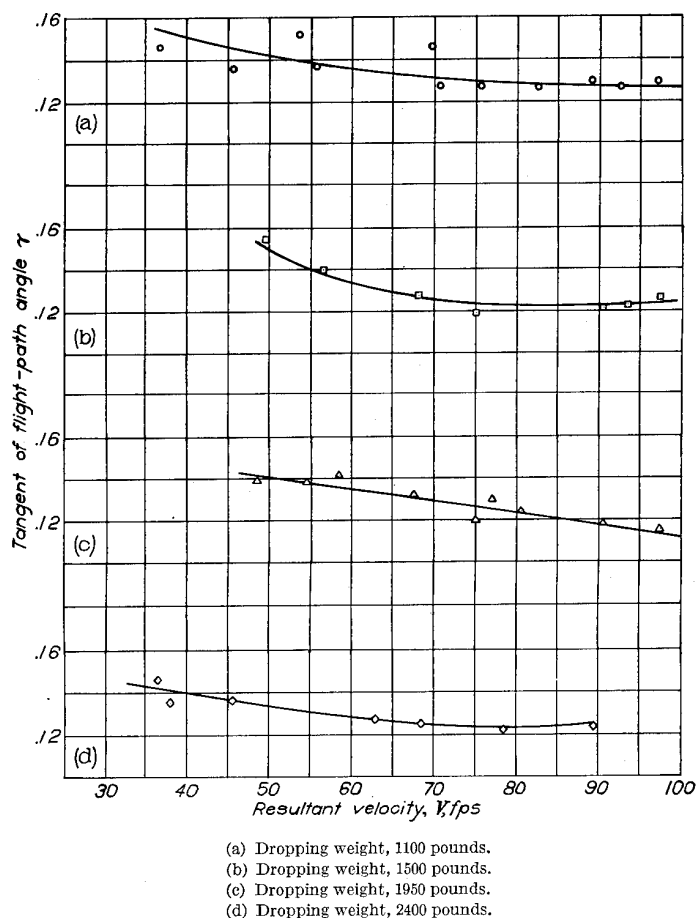


FIGURE 13.—Variation of flight-path angle with resultant velocity for various dropping weights.

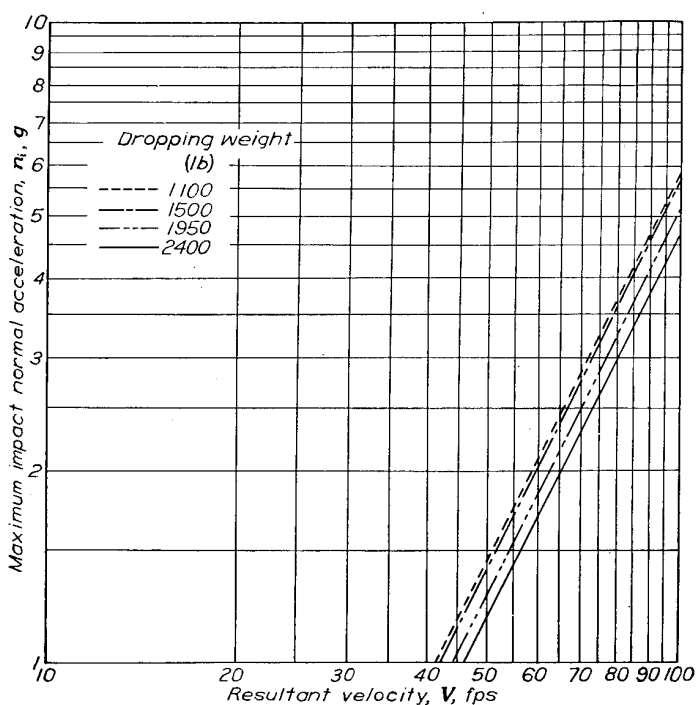


FIGURE 14.—Variation of maximum impact normal acceleration with resultant velocity for various dropping weights.

### CONCLUSIONS

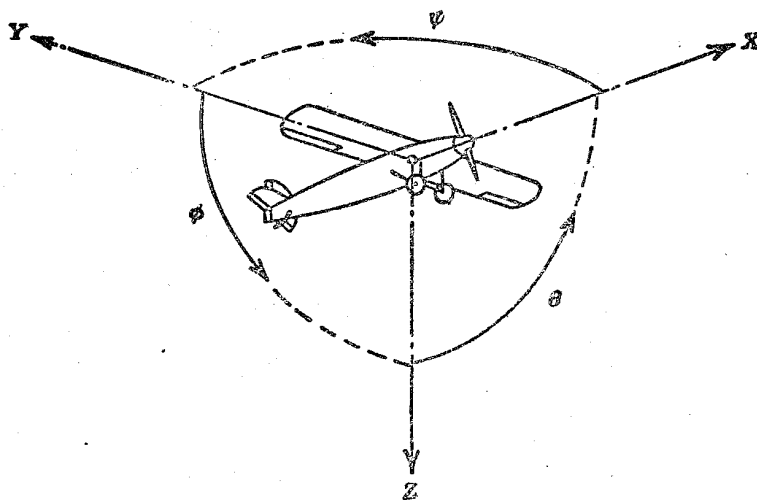
Results of tests in the NACA impact basin of the variation with resultant velocity and weight of the normal acceleration resulting from landings of seaplanes on water indicated the following conclusions:

1. The maximum impact normal acceleration was proportional to the square of the resultant velocity in accordance with the  $V^2$  law of fluid resistance.
2. The maximum impact normal acceleration decreased

as the weight increased provided all other conditions remained constant.

3. An increase in maximum impact normal acceleration accompanied an increase in flight-path angle provided all other conditions remained constant.

LANGLEY MEMORIAL AERONAUTICAL LABORATORY,  
NATIONAL ADVISORY COMMITTEE FOR AERONAUTICS,  
LANGLEY FIELD, VA., *June 2, 1944.*



Positive directions of axes and angles (forces and moments) are shown by arrows

| Axis              |             | Force<br>(parallel<br>to axis)<br>symbol | Moment about axis |             |                       | Angle            |             | Velocities                               |         |
|-------------------|-------------|--|-------------------|-------------|-----------------------|------------------|-------------|--|---------|
| Designation       | Sym-<br>bol |  | Designation       | Sym-<br>bol | Positive<br>direction | Designa-<br>tion | Sym-<br>bol | Linear<br>(compo-<br>nent along<br>axis) | Angular |
| Longitudinal..... | X           | X  | Rolling.....      | L           | Y→Z                   | Roll.....        | φ           | u  | p       |
| Lateral.....      | Y           | Y  | Pitching.....     | M           | Z→X                   | Pitch.....       | θ           | v  | q       |
| Normal.....       | Z           | Z  | Yawing.....       | N           | X→Y                   | Yaw.....         | ψ           | w  | r       |

Absolute coefficients of moment

$$C_l = \frac{L}{q b S} \quad C_m = \frac{M}{q c S} \quad C_n = \frac{N}{q b S}$$

(rolling)      (pitching)      (yawing)

Angle of set of control surface (relative to neutral position),  $\delta$ . (Indicate surface by proper subscript.)

#### 4. PROPELLER SYMBOLS

|       |   |        |   |
|-------|---|--------|---|
| $D$   | Diameter  | $P$    | Power, absolute coefficient $C_P = \frac{P}{\rho n^3 D^5}$            |
| $p$   | Geometric pitch   | $C_s$  | Speed-power coefficient $= \sqrt[5]{\frac{\rho V^5}{P n^2}}$          |
| $p/D$ | Pitch ratio   | $\eta$ | Efficiency  |
| $V'$  | Inflow velocity   | $n$    | Revolutions per second, rps   |
| $V_s$ | Slipstream velocity   | $\Phi$ | Effective helix angle $= \tan^{-1} \left( \frac{V}{2\pi r n} \right)$ |
| $T$   | Thrust, absolute coefficient $C_T = \frac{T}{\rho n^2 D^4}$ |        |   |
| $Q$   | Torque, absolute coefficient $C_Q = \frac{Q}{\rho n^2 D^5}$ |        |   |

#### 5. NUMERICAL RELATIONS

1 hp = 76.04 kg-m/s = 550 ft-lb/sec  
 1 metric horsepower = 0.9863 hp  
 1 mph = 0.4470 mps  
 1 mps = 2.2369 mph

1 lb = 0.4536 kg  
 1 kg = 2.2046 lb  
 1 mi = 1,609.35 m = 5,280 ft  
 1 m = 3.2808 ft